African Journal of Advanced Pure and Applied Sciences (AJAPAS)
Online ISSN: 2957-644X
Volume 5, Issue 1, 2026
Page No: 371-378
Website: https://aaasjournals.com/index.php/ajapas/index

ISI 2025: 1.126 SJIFactor 2024: 6.752 معامل التأثير العربي: 1.62

Performance Optimisation of Axial Field Partitioned Stator Switched Flux PM Machine with Spoke-type PM Stator

Mohammed F. H. Khatab [1*], Abubaker A. Saed [2]
[1,2] Electronics and Electrical Engineering, Faculty of Engineering, Omar Al-Mukhtar University, El-Bayda, Libya

تحسين الأداء لمحركات الفيض المحوري المتغير ذات العضو الثابت المنقسم عن طريق شكل المغناطيس الدائم في الجزء الثابت

محمد فرج خطاب [1*]، أبوبكر عطية سعد [2]
[2،1] قسم الهندسة الكهربائية والالكترونية، كلية الهندسة، جامعة عمر المختار، البيضاء، ليبيا

*Corresponding author: mohammed.khtab@omu.edu.ly

Received: December 03, 2025	Accepted: February 21, 2026	Published: March 05, 2026

Abstract
An axial field switched flux permanent magnet (AFSFPM) machine shows favourable production by integrating the benefits of both switched flux permanent magnet (SFPM) and axial field permanent magnet (AFPM) Machines. An axial-field partitioned stator switched-flux permanent magnet (AFPS-SFPM) machine was introduced, and the machine was optimised for maximum electromagnetic torque. This study examines the impact of PM shape on the performance of AFPS-SFPM machine. Surface-mounted PM was used for the basic machine stator. However, the machine is equipped with a flux-focusing permanent magnet stator (Spoke type stator). The design has been optimised and compared to the basic design. The results show that using a spoke-type PM stator significantly improved the machine's no-load performance. Moreover, the machine with spoke-type PM stator produces about 60% more torque than the machine with a surface-mounted PM stator. However, the proposed topology has a larger PM volume than the basic topology.

Keywords: Axial field, switched flux, partitioned stator, Permanent magnet, Spoke type stator.

الملخص
تتميز آلة المغناطيس الدائم ذي الفيض المحول المحوري (AFSFPM) بأداء جيد من خلال دمج مزايا كل من آلة المغناطيس الدائم ذي المجال المحوري (AFPM) وآلة المغناطيس الدائم ذي الفيض المحول (SFPM). تم تقديم آلة المغناطيس الدائم ذي الفيض المحول ذي المجال المحوري المقسم (AFPS-SFPM) وتم تحسينها بشكل فردي لتحقيق أقصى عزم دوران. تبحث هذه الدراسة تأثير شكل المغناطيس الدائم على أداء الآلة. تم استخدام مغناطيس دائم مثبت على السطح للجزء الثابت للآلة التقليدية. أضافة الى ذلك، تم تزويد الآلة بمغناطيس دائم مركز الفيض بالجزء ثابت (جزء ثابت من النوع المتشعب). تم تحسين التصميم الجديد ومقارنته بالتصميم التقليدي. بينت النتائج ان الآلة ذات الجزء الثابت المغناطيسي الدائم من النوع المتشعب تعطي عزم دوران أكبر من الآلة ذات الجزء الثابت المغناطيسي الدائم المثبت على السطح. علاوة على ذلك. فقد ثبت أن استخدام المغناطيس الدائم من نوع Spoke يحسن بشكل كبير من أداء الألة بدون حمل. ومع ذلك، فإن الماكينة ذات التركيب المقترح لها حجم مغناطيس أكبر من التركيب الأساسي.

الكلمات المفتاحية: الفيض المحوري، الجزء الثابت المنقسم للمحرك، محركات الفيض المتغير، محركات المغناطيس الدائم.

Introduction

Axial field permanent magnet (AFPM) machines have recently emerged as more suitable options for diverse applications [1]. Their disk-shaped profile and short axial length make them particularly suitable for integration into confined spaces, such as those found in electric vehicles, wind turbines, and aerospace applications [2]. Moreover, among AFPM topologies, the Spoke-type rotor is used in permanent magnet machines. One benefit of this design is that it can achieve a high air-gap flux density due to the effect of PM flux focusing [3, 4].

Recently, a Partitioned stator structure has been presented in [5]. The results showed that the electromagnetic torque of permanent magnet machines can be improved by employing a partitioned stator (PS-SFPM), which provides additional space within the inner rotor. Compared to the traditional SFPM machine, the PS-SFPM design produces greater torque. The partitioned stator concept, by physically separating armature windings and permanent magnets onto distinct stator sections, effectively mitigates the conflict between electric and magnetic loadings, thereby enabling simultaneous realisation of high torque density and energy-efficient flux control [5]. Additionally, the axial flux is also designed with a partitioned stator. The axial flux (AF) PS-SFPM machine features two distinct stators, each serving different roles. An AFPS-SFPM machine was first presented in [6]. Moreover, for maximum torque and minimum torque ripple, the machine was optimised in [7].
In this article, the AFPS-SFPM machine with a spoke-type stator is designed and simulated. Moreover, the structure of both the basic topology (with surface-mounted PM stator) and the proposed topology (with spoke-type stator) is explained, and the parameter definitions are presented. Furthermore, the PM thickness of the proposed design is individually optimised to study the impact of changing the PM on the stator on the machine performance. Finally, a performance compression of the basic and the proposed machines is carried out.

Machine Geometry

The basic 2D and 3D configurations of 12 stator windings, 10-pole, 3- phase AFPS-SFPM machine, is indicated in Figure 1, which was presented and optimised in [1]. The rotating part of the machine is made of iron parts and is situated between two separate stators. Consequently, the machine has a passive iron and rigid rotating part similar to that of the switching reluctance motor. Additionally, the stator comprises two totally separate parts. The first part, referred to as the armature stator, has 12 focused coils wrapped around the adjacent teeth. The 3-phase stator windings are double-layer distribution, each phase consists of four coils. The stator coils are arranged in series to form the stator phase windings. In addition, the armature stator pole numbers n_s and the rotor pole-pair number p Combinations are expressed by [2]:

$$n_s = 2p \pm k,\ \ k = 1,2,\dots \quad (1)$$

It has been provided that high flux and balanced magnetic pull can be obtained when $k = 2$,. The second part is known as the excitation stator, which contains 12 PMs located at the inner surface of the core (surface-mounted) that are pre-magnetised in the opposite direction. As a result, the center lines of the permanent magnets in the excitation stator align with the teeth of the armature stator, and both stators share the same number of poles and teeth.

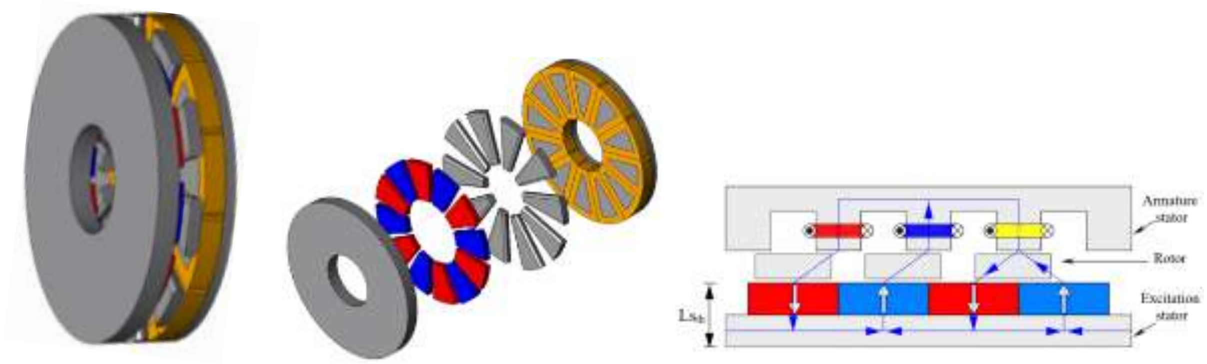

(a) (b)

Figure 1 The basic configuration. (a) 3D view (b) Cross-Cutting view.

Since the basic topology was optimised in [1], the proposed topology will be redesigned with a flux focusing PM stator (Spoke type stator) and with the same stator and rotor as the basic topology, as presented in Figure 2. Both topologies are designed utilising (Jmag) 3-D finite element analysis (FEA) software [3]. The influence of the PM thickness on the machine performance will be examined. which is a significant issue throughout PM machine design procedure. The induced EMF phasor in each coil can obtain the distribution of the coils of each phase [4]. The coil distribution for 12 armature stator poles is illustrated in Figure 3. In addition, the main parameters and materials of the machine topologies are presented in Table 1.

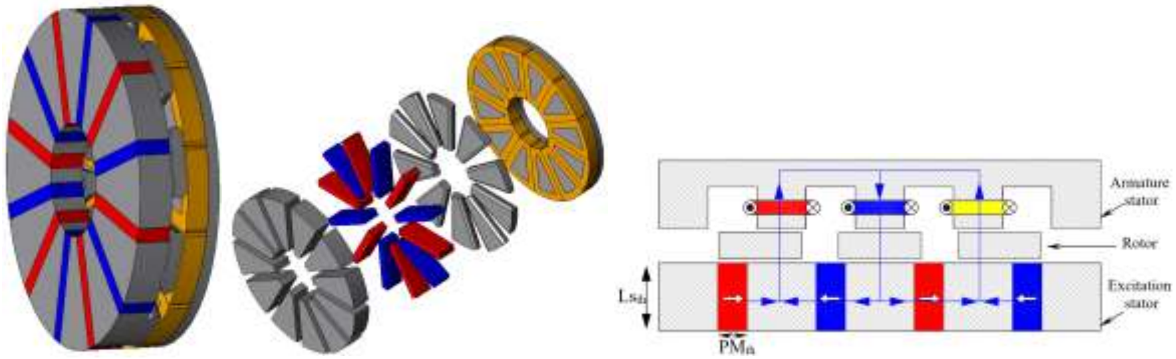

(a) (b)

Figure 2 The proposed configuration. (a) 3D view (b) Cross-Cutting view.

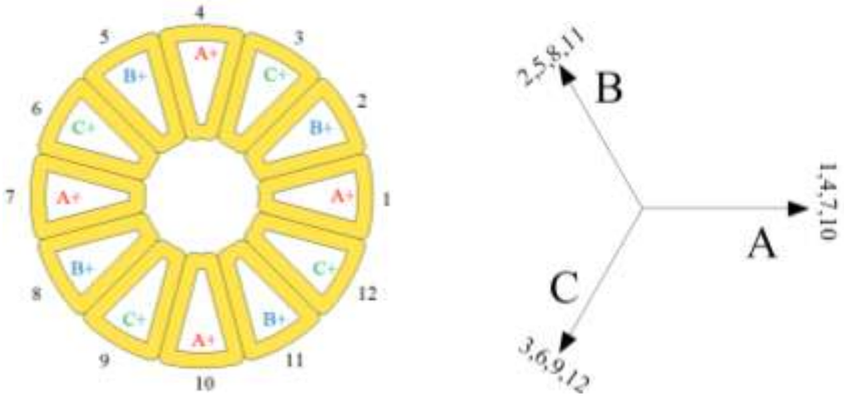

Figure 3 Coil arrangements and the EMF phasor.

Table 1 Machines Parameters, and Materials

Parameter	Value
Rotating Speed (rpm)	300
Stator Poles	12
Rotor Poles	10
Total Axial Length (mm)	25
Inner Radius (mm)	15
Outer Radius (mm)	45
Airgap Length (mm)	0.5
Fill Factor	0.5
Copper Loss P_{cu} (W)	10
RMS Current $I_{a\ RMS}$ (A)	5.5
Permanent magnet Material	NdFeB
Permanent magnet remanence B_r (T)	1.2
Permanent magnet relative permeability (μ_r)	1.05
Core Material	GKN SMC 70H

Impact of the thickness of PM on the Proposed Machine Performance

To examine the influence of the PM thickness on the torque of the proposed machine, the excitation stator thickness ($L\ s_{th}$) is kept the same as the basic model [5]. The considered average torque and the matching torque ripple for the proposed topology at different stator PM (PM_{th}) thickness are examined. The torque ripple can be calculated with reference to the average torque [6].

$$T_{\text{ripple}} = \frac{T_{\max} - T_{\min}}{T_{\text{avg}}} \% \qquad (2)$$

Where: T_{avg} is the average electromagnetic torque, T_{Max} and T_{Min} are the maximum and minimum electromagnetic torques, respectively.

The influences of average torque and torque ripple with the excitation stator PM thickness are shown in Figure 4. Both electromagnetic torque and torque ripple are highly proportional to the PM thickness. The average torque increases sharply with PM thickness, and the maximum torque with minimum torque ripple can be achieved when the PM thickness is about 7 mm. Moreover, the open circuit induced EMF of the stator windings is also increased as the PM thickness increases and attains its optimal value of about 2.6 V at PM thickness of 7 mm, as indicated in Figure 5. Therefore, this value is determined as the optimal value of the PM thickness of the proposed topology.

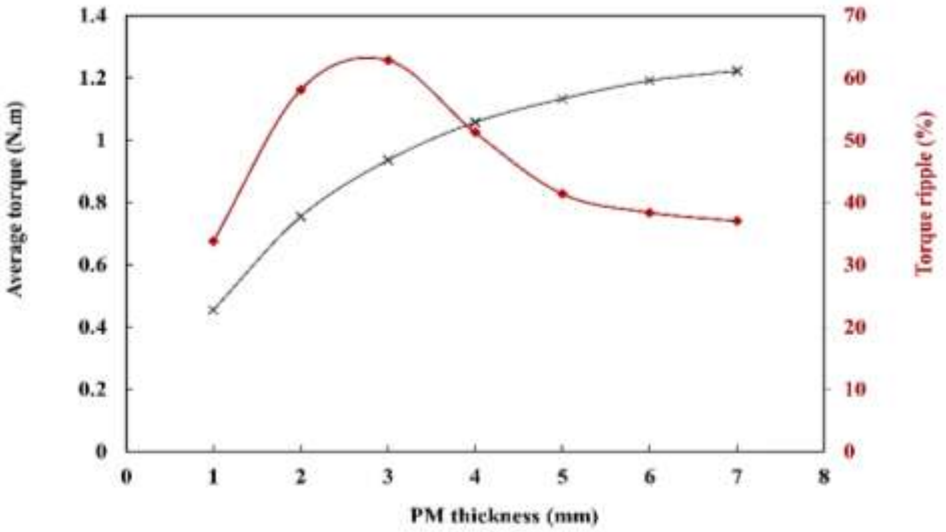

Figure 4 The characteristics of effect of stator PM thickness on the average torque and torque ripple

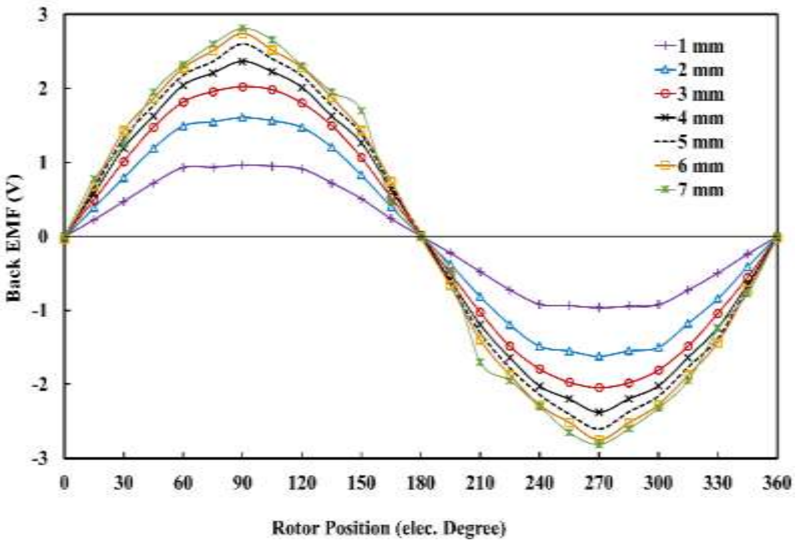

Figure 5. Back EMF against PM thickness characteristics.

No- load performance comparison between basic and proposed topologies

The no-load performance of both topologies is simulated and compared. Figure 6 and Figure 7, Display the EMF with its harmonic spectra and the air-gap flux density waveforms of the compared topologies, respectively. The no-load flux density generated by the magnet is one of the most crucial for examining the PM machine behavior. Clearly, the topology with spoke PM stator has significantly higher peak no-load EMF and flux linkage of about 2.6 V, and 8 mWb, respectively. This result is due to the flux in the gap being increased with the new PM arrangement.

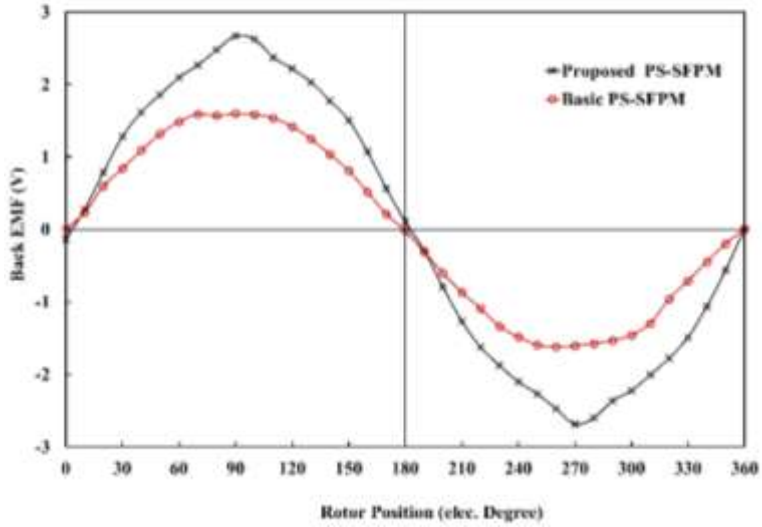

(a) Waveforms

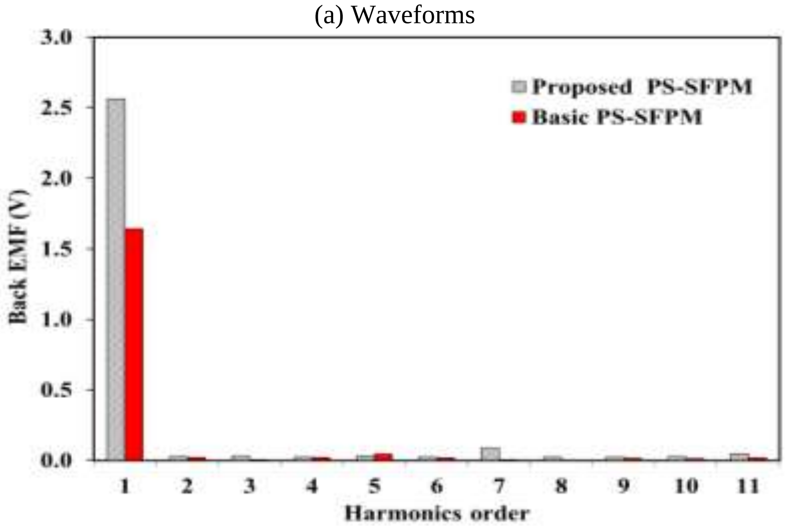

(b) Harmonics Spectra

Figure 6 Comparison of the no-load back EMF of the topologies.

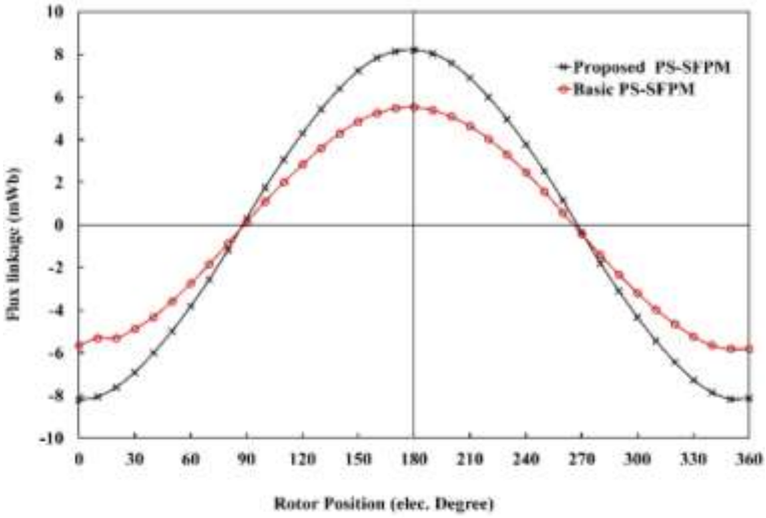

Figure 7 Comparison of the no-load flux linkage of the topologies.

On- load performance comparison between basic and proposed topologies.

To compare the on-load performance of both topologies, a rated current is injected into the stator windings. Figure 8 presents the electromagnetic torque of both topologies. It can be shown that the electromagnetic torque performance is significantly improved by the spoke PM arrangement. It is shown that using this arrangement in the stator results in an increase in the average electromagnetic torque of about 60%. Nevertheless, the basic model has a lower torque ripple of about 17% compared with the proposed machine in which the torque ripple is increased to 33 % for the proposed model.

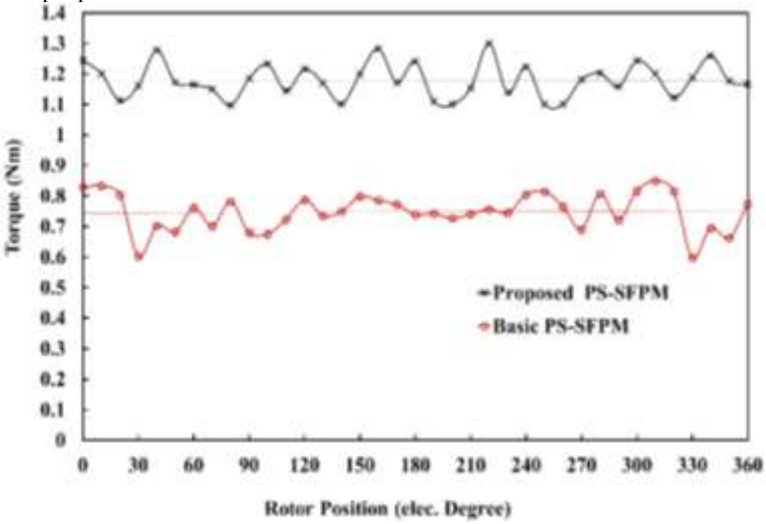

Figure 8 The average torque characteristics of the compared topologies.

Moreover, the electromagnetic torque characteristic at different currents, current density and windings copper loss was also simulated and compared. Figure 9, shows the torque with different current characteristics. The figure shows that, the proposed topology has better characteristic compared to the basic model. Moreover, the torque characteristic at different current density and copper loss of both topologies are studied and compared in Figure 10 and Figure 11, respectively. When the end winding is neglected, the winding resistance R_a per phase and the copper loss P_{cu} can be given by:

$$R_a = \frac{n \times 2\rho \; L_a N_a^2}{A_a \; k_{pf}} \qquad (2)$$

$$P_{cu} = {I_{a\,RMS}}^2 \times 3 \; R_a \qquad (3)$$

where, n is the number of coils per phase, N_a is the number of winding turns per phase, ρ is the copper resistivity, L_a is the coil active length, A_a is the coil area, k_{pf} is the winding fill factor, and $I_{a\,RMS}$ is the root mean square of the phase current. The comparison shows that the proposed model has improved average torque and torque-copper loss characteristics compared to the basic model. This improvement is due to the leakage flux being higher for the basic topology than for the proposed one.

Moreover, further study is carried out for the topologies. Figure 12 presents the topologies' torque density at different current, while Figure 13 shows the current per PM volume at different RMS current. It should be mentioned that the torque density is the electromagnetic torque divided by the machine volume. The figures show that the proposed topology has a superior torque density compared with the basic model at different RMS current. However, the topology with surface-mounted PM stator has better torque per magnet volume since more magnet material is utilised in the Spoke type stator machine.

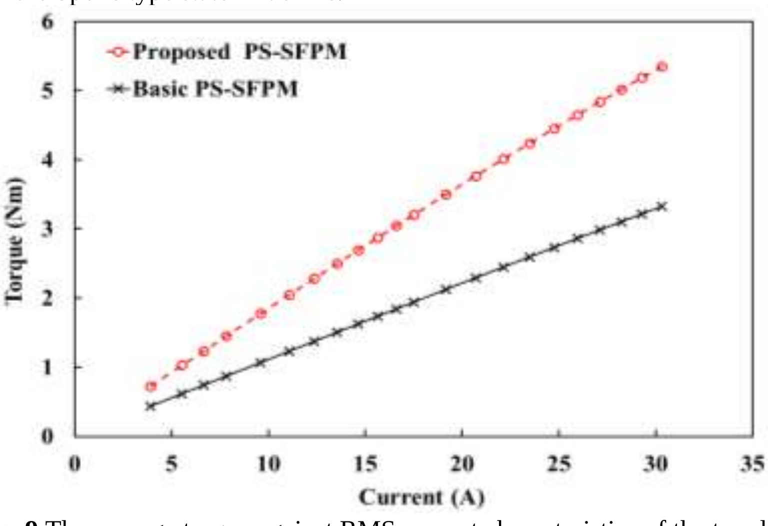

Figure 9 The average torque against RMS current characteristics of the topologies.

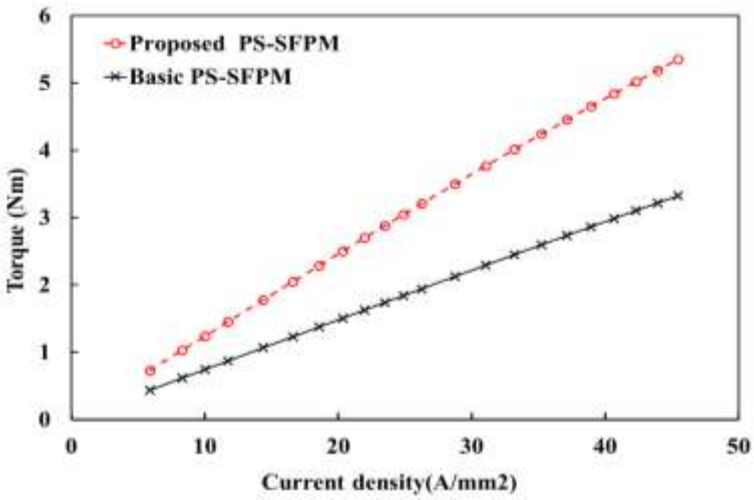

Figure 10 The average torque against current density characteristics of the topologies.

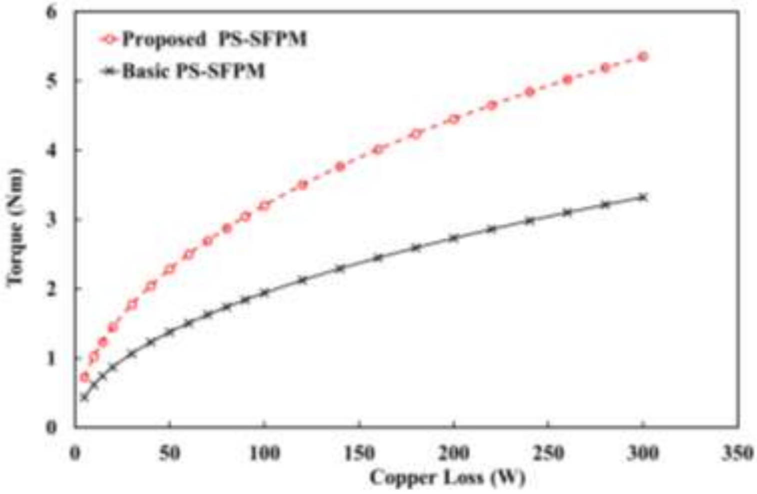

Figure 11 The average torque against copper loss characteristics of the topologies.

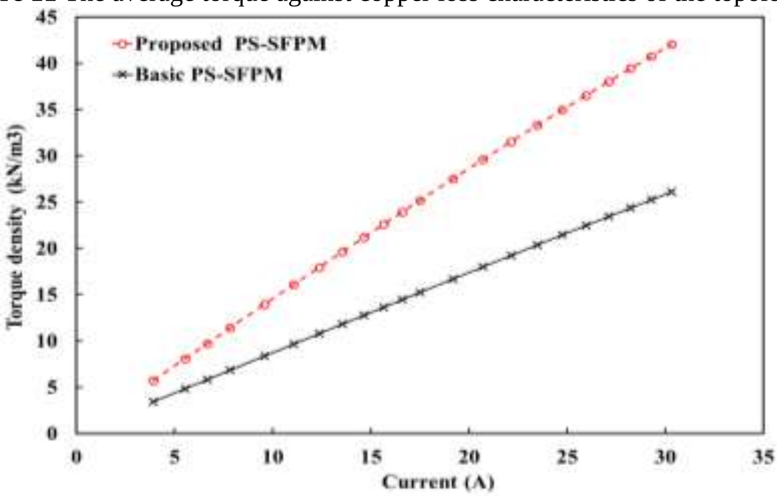

Figure 12 The torque density against RMS current characteristics of the topologies.

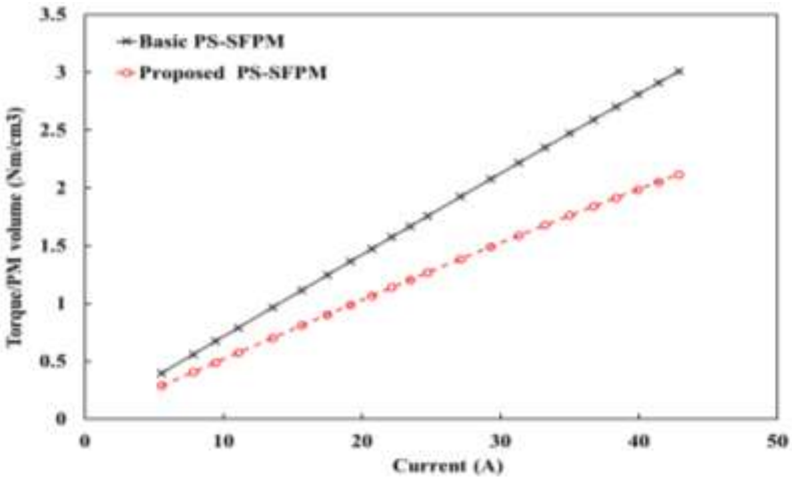

Figure 13 The torque per magnet volume against RMS current characteristics of the topologies.

Conclusion

In this paper, the performance of AFPS-SFPM machine topology was improved by changing the stator PM arrangement using 3D-FEA software. Flux focusing PM has been chosen to form the new stator shape (Spoke-type stator). The impact of the PM thickness on the machine performance was investigated. The machine torque increases when the PM is increased. Moreover, it is found that AFPS-SFPM topology with spoke type stator has significant performance compared to the basic topology. Furthermore, the machine electromagnetic torque and no-load EMF are both increased by approximately 60 % when a Spoke-type stator is employed.

Compliance with ethical standards

Disclosure of conflict of interest

The author(s) declare that they have no conflict of interest.

References

[1] M. F. Khatab, A. L. Shuraiji, and Z. Q. Zhu, "Parametric design optimization of axial field partitioned stator switched flux PM machine," in *2015 International Conference on Sustainable Mobility Applications, Renewables and Technology (SMART)*, 23-25 Nov. 2015 2015, pp. 1-6, doi: 10.1109/SMART.2015.7399216.

[2] D. Ishak, Z. Q. Zhu, and D. Howe, "Permanent-magnet brushless machines with unequal tooth widths and similar slot and pole numbers," *IEEE Transactions on Industry Applications*, vol. 41, no. 2, pp. 584-590, 2005, doi: 10.1109/TIA.2005.844380.

[3] "Jmag Designer software." https://www.jmag-international.com/.

[4] M. Aydin, Z. Q. Zhu, T. A. Lipo, and D. Howe, "Minimization of Cogging Torque in Axial-Flux Permanent-Magnet Machines: Design Concepts," *Magnetics, IEEE Transactions on*, vol. 43, no. 9, pp. 3614-3622, 2007, doi: 10.1109/TMAG.2007.902818.

[5] Z. Q. Zhu and X. Liu, "Individual and global optimization of switched flux permanent magnet motors," in *Electrical Machines and Systems (ICEMS), 2011 International Conference on*, 20-23 Aug. 2011 2011, pp. 1-6, doi: 10.1109/ICEMS.2011.6073806.

[6] Z. Z. Wu, Z. Q. Zhu, and J. T. Shi, "Novel Doubly Salient Permanent Magnet Machines With Partitioned Stator and Iron Pieces Rotor," (in English), *Ieee T Magn*, vol. 51, no. 5, pp. 1-12, May 2015, doi: Artn 8105212 . 10.1109/Tmag.2015.2404826.

